

Further Model Experiments of the Combined Effect of Aft-Body Forms and Propeller Revolutions upon the Propulsive Economy of Single-Screw Ships.

By **Masao Yamagata**, of the Teishinsho Ship Experiment Tank,
Kogakushi, Member.

Introduction.

In general, the under-water forms of ships are determined without regard to the number of revolutions of the propeller to be fitted, and some designers even go so far as to determine them only from the resistance point of view. I believe, however, in order to obtain the highest propulsive economy of single-screw full-lined ships, the aft-body forms should, as a matter of course, be designed in conjunction with the propeller revolutions.

In view of the lack of the information concerning such a combined effect of aft-body forms and propeller revolutions upon the propulsive economy, systematic model experiments are being conducted at the Teishinsho Ship Experiment Tank in Tokyo, with the object of obtaining the information applicable to about 120-metre single-screw cargo ships. As the first report of this experimental investigation, I presented a paper⁽¹⁾ at the summer meeting of the Institution of Naval Architects held in 1934, which dealt with the combined effect of the frame-line shape, i.e. the vertical distribution of the displacement, of aft-body forms and propeller revolutions. The present paper, the second report of this research, discusses the interrelation between the longitudinal distribution of the displacement of aft-body forms and propeller revolutions from the propulsion point of view.

Ship Models Employed.

The experiments were carried out on three ship models, i.e. Nos. 195, 319 and 320, which represented 120-metre single-screw full-lined cargo ships of fairly normal

⁽¹⁾ Trans. Inst. N. A., 1934.

forms with raised sterns, intended to run at about 14 knots, when fully loaded. These were made to a scale of 1:20 in paraffin wax, and their leading particulars were as follow :—

Length between perpendiculars	6.000 m.
Breadth extreme	0.800 m.
Load draught	0.355 m.
Load displacement	1,265.6 kg.
Block coefficient... ..	0.743
Longitudinal prismatic coefficient	0.754
Midship section coefficient.....	0.986

These models had the same form of fore-body and similar shape of aft-body frame-line, and the difference was confined to the longitudinal distribution of the displacement of aft-body, the longitudinal position of the centre of buoyancy of models Nos. 319, 195 and 320 being 6.43cm., 7.44cm. and 8.09cm. forward from midship section, respectively. Fig. 1 shows their sectional area curves and load water-lines. They were fitted with all appendages except bilge keels, which might when not properly located, confuse the conclusions of the present research. The body-plans, together with the bow and stern arrangements, are illustrated in Fig. 2.

Resistance Tests.

As I emphasized in the previous paper, the resistance tests, which are universally carried out at experiment Tanks, are useless and misleading for single-screw full-lined ships, because the form of the least towing resistance does not show the best propulsive performance under the given conditions. In the present research, however, resistance tests were made with the peculiar object of demonstrating how they were of no use for such ships.

Each ship model was run in smooth water on level trim at the load displacement to ascertain its resistance. In Fig. 3 the results are plotted in our standard non-dimensional form, and in Fig. 4 three effective horse-power curves for 120-m. ships, calculated from the results shown in Fig. 3 by Froude's skin friction constants corrected to the standard temperature of 15°C. to clean-ship condition in salt water without any allowance for wind and wave resistances, are given on a base of speed in knots. It will be seen from Fig. 4 that the effective horse-power curves of models Nos. 195 and 319 completely coincide and that of model No. 320 is a little higher than the others over a range of working speed.

Wake Tests.

In order to obtain the necessary information for designing propellers, the mean annular wake distributions at the propeller position were measured on each ship model at a model speed of 1.6 m./sec., corresponding to 13.9 knots for 120-m. ships, by means of thirteen blade-wheels of mean radii from 2.5 to 14.5 cm. These measurements were made under the same conditions as those at the resistance tests, with an exception that the rudder was removed from each model to simplify the experimental arrangement. In Fig. 5 these test results are shown in the form of mean annular wake fraction, expressed in terms of model speed, on a base of the radius of annular ring. It will be observed that the fuller the after part of hull the larger the wake fraction.

In Appendix II, comparing the mean wake fractions over propeller discs, derived from these measurements, with those obtained by Froude's method of propeller analysis, I will discuss the discrepancy between these two kinds of mean wake fractions, and show how we can, when necessity calls, calculate the approximate value of the latter directly from the measured mean annular wakes, without conducting propeller open-water tests.

For the purpose of obtaining the wake at every point over propeller discs, the similar tests were repeated, using pitot tubes instead of blade-wheels. Fig. 6 shows the equi-wake lines at the propeller position of each model at a speed of 1.6 m./sec., and Fig. 7 gives the peripheral variations of wakes at the radii of 6.5, 8.5 and 10.5 cm. From these two figures, we know that the wake distributions of models Nos. 195, 319 and 320 may be said to be quite similar, though, as stated in the above, the absolute values of wake fractions are affected by the longitudinal distribution of the displacement of aft-body.

Propeller Models Employed.

Four speeds of propeller revolutions at 3,000 S.H.P. were aimed at for each 120-m. ship, namely, 70, 100, 130 and 160 per minute. All the propellers were of the four-bladed and similar type with aerofoil sections, the expanded area ratio being 0.407, the blade thickness ratio 0.045, and the boss diameter 4.8 cm., paying, for the sake of simplicity, no special consideration to strength, cavitation, etc., for full-sized propellers.

To obtain the necessary information for designing propellers, preliminary self-propulsion tests were carried out on each ship model with each of its four propeller models, which had been selected as the most suitable for the present requirements among our standard series propellers and the other propeller models on hand.

Examining these twelve test results, the speed of each model corresponding to that of 120-m. ship at 3,000 S.H.P. and thrust deduction fraction were assumed for each propeller model to be designed. Next, since the mean annular wake fractions are nearly constant over a certain range of model speed, the measured results at a model speed of 1.6 m./sec., given in Fig. 5, were considered as those at the assumed attainable speeds, which ranged from 1.55 to 1.64 m./sec.

Using these data, i.e. the attainable speeds, thrust deduction fractions and mean annular wake fractions, four propellers for each ship model, making twelve in all, were designed by the normal method⁽²⁾ at our Tank, not allowing for so-called "scale effects" between ships and models. The dimensions and particulars are tabulated below.

Propeller Number.	R.P.M. aimed at.	Diameter in cm.	Pitch Ratio (Variable) at 0.7R.	For Ship Model Number.
155	70	29.92	0.943	195
156	100	24.88	0.820	195
157	130	21.89	0.720	195
158	160	19.92	0.638	195
174	70	29.86	0.927	319
175	100	25.27	0.815	319
176	130	22.30	0.709	319
177	160	20.40	0.613	319
178	70	29.95	0.946	320
179	100	24.83	0.818	320
180	130	21.77	0.714	320
181	160	19.80	0.619	320

The general plans of propellers Nos. 174 to 181 are given in Figs. 8 to 15, and those of propellers No. 155 to 158 were given in the previous paper.

Self-Propulsion Tests.

Under the same conditions as those at the resistance tests, each ship model was tested, self-propelled with each of its four propellers, by our normal method of self-

⁽²⁾ A. Shigemitsu, Report of the Teishinsho Ship Experiment Tank, 1931.

propulsion tests, namely, at what is known as the ship point of self-propulsion, not allowing for bilge keels, foul bottom, wind, wave, etc. Figs. 16 to 18 give the results of these twelve self-propulsion tests in our standard non-dimensional form, and in Figs. 19 to 21 the S.H.P., R.P.M. and propulsive coefficient curves for 120-m. ships are shown on a base of speed in knots. As seen in these figures, the propeller revolutions at 3,000 S.H.P. do not exactly coincide with those aimed at, hence, in Fig. 22, the attainable speeds and propulsive coefficients associated with the thrust deduction fractions at 3,000 S.H.P. are plotted on a base of R.P.M., and three fair curves are drawn for each ship model. Moreover, in order to facilitate the discussion of the test results, in Fig. 23 these speeds and coefficients read from Fig. 22 for the definite revolutions from 70 to 160 per minute, together with the mean thrust deduction fractions over the tested range of propeller revolutions are shown on a base of the relative longitudinal position of centre of buoyancy l_{cb} , i.e. the ratio of the longitudinal distance of centre of buoyancy from midship section to the length of ship.

Conclusions.

From Fig. 23, which summarizes the test results, the following conclusions will be drawn :—

(a) When propeller revolutions are low, both the attainable speeds and propulsive coefficients at 3,000 S.H.P. for the same revolutions quickly increase at first and then gradually fall off with the forward shift of centre of buoyancy, while, in the case of high revolutions, the finer the after part of hull, the better the propulsive performance.

(b) As propeller revolutions increase, the optimum position of centre of buoyancy shifts forward materially. Comparing this experimental result with that described in the previous paper, it can be said that for the purpose of obtaining the highest propulsive economy the longitudinal distribution of the displacement of aft-body is far important than its vertical distribution.

(c) The adoption of large slow-running propellers always improves the propulsive performance, though the rate of improvement varies with the variation of the longitudinal distribution of the displacement of aft-body.

(d) Though the thrust deduction fraction for a definite form of hull may be said to be approximately constant over a wide range of propeller revolutions, it changes materially with the variation of the longitudinal distribution of the dis-

placement of aft-body, namely, it quickly at first and then gradually falls off with the forward shift of centre of buoyancy.

It should be remembered that these conclusions cannot be absolutely true, unless all the propellers employed were the optimum under the given conditions. Experience has shown that the propellers designed by our method may be generally said to be quite close to the optimum, though, strictly speaking, they may not be the optimum. Therefore, I firmly believe that the above conclusions can apply approximately to all ships similar to those dealt with in the present paper.

In Appendix III, according to the current practice at experiment Tanks, the results of the present self-propulsion tests are analysed by Froude's method, which would be useful to other Tank experimenters for comparing these results with their own data.

Appendix I.

Symbols Used.

Symbol	Dimensions.			Remarks.
	kg.	m.	sec.	
ρ	1	-4	2	Density, i.e. mass of unit volume, of water.
L	0	1	0	Length of ship.
V	0	1	-1	Speed of ship.
V'				Speed of ship in knots.
R	1	0	0	Resistance of ship.
R_f	1	0	0	Frictional resistance.
R_w	1	0	0	Wave-making resistance.
∇	0	3	0	Immersed volume.
g	0	1	-2	Gravitational acceleration.
$v = \frac{V}{\nabla^{\frac{1}{3}} g^{\frac{1}{2}}}$	0	0	0	Relative speed.
$r = \frac{R}{\rho \nabla^{\frac{2}{3}} V^2}$	0	0	0	Relative resistance.

$r_f = \frac{R_f}{\rho \nabla^{\frac{2}{3}} V^2} \dots 0$	0	0	Relative frictional resistance.
$r_w = \frac{R_w}{\rho \nabla^{\frac{2}{3}} V^2} \dots 0$	0	0	Relative wave-making resistance.
E.H.P.			Effective horse-power.
$N \dots 0$	0	-1	Revolutions of propeller.
$T \dots 1$	0	0	Thrust of propeller.
$Q \dots 1$	1	0	Torque of propeller.
$n = \nabla^{\frac{1}{3}} \frac{N}{V} \dots 0$	0	0	Relative revolutions.
$t = \frac{T}{\rho \nabla^{\frac{2}{3}} V^2} \dots 0$	0	0	Relative thrust.
$p = \frac{2\pi NQ}{\rho \nabla^{\frac{2}{3}} V^3} \dots 0$	0	0	Relative power.
S.H.P.			Shaft horse-power.
$\eta = \frac{\text{E.H.P.}}{\text{S.H.P.}} \dots 0$	0	0	Propulsive coefficient.

Note.--The suffixes "m" and "s," representing "model" and "ship" respectively are added to the above symbols, when necessity calls.

Appendix II.

On the Mean Wake.

Since, at our experiment tank, we always design propellers every annular element, taking the corresponding mean annular wake at the propeller position, which has been measured by a blade-wheel, into consideration, it is unnecessary for us to know the mean wakes over propeller discs, which, in accordance with the current practice at experiment Tanks, are obtained by Froude's method of propeller analysis, i.e. comparing the results of self-propulsion tests with those of propeller open-water tests, and are used for the design of propellers by means of the propeller design diagrams which summarized the results of systematic model propeller experiments in open water. Moreover, it may be said that open-water tests are useless to our propellers thus designed, i.e. so-called "wake

propellers." From these two reasons propeller open-water tests are, as a general rule, not carried out at our Tank. Therefore, I want to avail myself of the present occasion to consider briefly the discrepancy between the following two kinds of mean wakes, and to show how we can, when necessity calls, obtain the approximate value of the mean wake fraction, which is used for analysing a propulsive coefficient by Froude's method, directly from the measured mean annular wakes, without conducting propeller open-water test.

The mean wake over a propeller disc, which is used for discussing the interaction between ship and propeller, may be classified into (a) "nominal mean wake," which is obtained by integrating the wakes measured by pitot tubes or blade-wheels over a propeller disc, and (b) "effective mean wake," which is usually determined by conducting open-water tests. The main difference between these two kinds of mean wakes may be said to be whether they are independent or dependent of the thrust distribution over propeller blade. In spite of such an essential difference, these two are often dealt with as if they were comparable. I will, therefore, calculate these mean wake fractions, and show how their calculated values are different.

To obtain the nominal mean wake fraction over a propeller disc from the wakes measured by pitot tubes or blade-wheels, two different methods of calculation are generally adopted; one is so-called "method of volume-integration," and the other "method of momentum-integration." When wake measurements have been made by pitot tubes, this fraction based upon the former method is

$$w_v = \frac{\iint w_0 r d\theta dr}{\iint r d\theta dr}, \dots\dots\dots (1)$$

and that based upon the latter is

$$w_m = \frac{\iint w_0 (1 - w_0) r d\theta dr}{\iint (1 - w_0) r d\theta dr}, \dots\dots\dots (2)$$

where w_0 is the wake fraction at any point over a propeller disc. When blade-wheels have been employed, the mean wake fractions based upon the former and latter methods are expressed by

$$w_v = \frac{\int w' r dr}{\int r dr} \dots\dots\dots(1')$$

and

$$w_m = \frac{\int w'(1-w') r dr}{\int (1-w') r dr} \dots\dots\dots(2')$$

respectively, where w' is the mean annular wake fraction measured by a blade-wheel. But, since a blade-wheel can be considered as an instrument of obtaining the mean annular wake by the momentum-integration of wakes over an annular ring, it may be said that the expression of (1') should not be used for the purpose of the radial integration of the mean annular wake fractions measured by blade-wheels.

From the measured mean annular wake fractions shown in Fig. 5, the nominal mean wake fractions, w_v and w_m , were calculated by the expressions of (1') and (2'), and are given in Figs. 24 and 25, respectively, on a base of the relative longitudinal position of centre of buoyancy l_c . It will be found from these figures that the values of w_v are always greater than those of w_m . Again, in order to facilitate for obtaining the nominal mean wake fractions over the propeller discs of any diameter, in Figs. 26 and 27 these values were presented on a base of the radius of circular disc; from which the nominal mean wake fraction over each circular disc of the twelve propellers employed in the present research was read and tabulated in the annexed table.

As stated before, the nominal mean wake fractions, w_v and w_m , thus obtained differ with the effective mean wake fraction w_a , which is employed in Froude's method of propeller analysis adopted universally at experiment Tanks, and can be expressed by

$$w_a = 1 - \frac{V_a}{V} = 1 - \frac{\text{T.H.P.}}{T \cdot V} \dots\dots\dots(3)$$

where V = speed of ship,

V_a = effective mean speed of advance of propeller, which can be obtained by comparing the result of self-propulsion test with that of propeller open-water test,

T = thrust of propeller,

and T.H.P. = thrust horse-power.

Comparison of Mean Wake Fractions.					
Model No.	Propeller No.	Nominal mean wake fractions.		Effective mean wake fractions.	
		w_v	w_m	w_a	w_c
319	174	.37	.34	.41	.40
195	155	.33	.30	.37	.36
320	178	.31	.29	.34	.33
319	175	.43	.40	.47	.46
195	156	.39	.36	.42	.42
320	179	.36	.34	.39	.38
319	176	.47	.45	.52	.50
195	157	.43	.40	.50	.46
320	180	.40	.38	.45	.42
319	177	.51	.48	.59	.53
195	158	.46	.44	.52	.48
320	181	.42	.41	.43	.45

All the propellers employed in the present research were tested in open water, and by Froude's method the effective mean wake fractions w_a at the attainable speeds at 3,000 S.H.P. of 120-m. ships were found, whose figures are given in the previous table.

But the approximate value of this fraction can be calculated directly from the measured mean annular wakes.

According to the momentum theory of the action of a screw propeller, the thrust and thrust horse-power in the expression of (3) may be written as follows:—

$$T = 2\pi\rho \int_{R_0}^R kr \left(V_{ra} + \frac{1}{2} U_{ra} \right) U_{ra} (1 - \varepsilon \operatorname{tg} \beta_{ri}) dr$$

and

$$\text{T.H.P.} = 2\pi\rho \int_{R_0}^R kr V_{ra} \left(V_{ra} + \frac{1}{2} U_{ra} \right) U_{ra} (1 - \varepsilon \operatorname{tg} \beta_{ri}) dr,$$

where ρ = density of water,

r = radius at any section of propeller blade,

R = tip radius of propeller,

R_0 = radius of propeller boss,

V_{ra} = mean annular speed of advance at the radius r ,

U_{ra} = induced mean annular axial velocity at a great distance behind propeller,

ε = fineness expressing skin friction,

β_{ri} = induced pitch angle at the radius r ,

and

k = Prandtl's factor of modification for a definite number of propeller blades

$$= \frac{2}{\pi} \cos^{-1} e^{-\frac{\pi}{2} \left(1 - \frac{r}{R}\right) \operatorname{cosec} \beta_i},$$

z = number of blades,

β_i = induced pitch angle at the tip.

Then, denoting the calculated effective mean wake fraction by w_c , to distinguish this from that obtained by conducting propeller open-water test, the expression of (3) becomes

$$w_c = 1 - \frac{\int_{R_0}^R kr V_{ra} \left(V_{ra} + \frac{1}{2} U_{ra} \right) U_{ra} (1 - \varepsilon \operatorname{tg} \beta_{ri}) dr}{V \int_{R_0}^R kr \left(V_{ra} + \frac{1}{2} U_{ra} \right) U_{ra} (1 - \varepsilon \operatorname{tg} \beta_{ri}) dr} \dots \dots \dots (4)$$

For the propellers designed by our method, this equation can easily be solved graphically at their designed speeds. The effective mean wake fractions w_c thus obtained are also given in the previous table.

In this table the speeds at which mean wake fractions were obtained are not identical, namely, the nominal mean wake fractions, w_n and w_m , were calculated at a model speed of 1.6 m./sec., which corresponds to 13.9 knots for 120-m. ships, and the effective mean wake fractions, w_a and w_c , were obtained at the attainable speeds at 3,000 S.H.P. of 120-m. ships and propeller designed speeds, respectively. But, since wake fractions are nearly constant over a certain range of model speed, the mean wake fractions obtained above may be considered to be accurately comparable. Then, it will be said from this table that the effective mean wake fractions are always greater than the nominal mean wake fractions, and that the effective mean wake fractions calculated by the expression of (4) are approximately equal to the measured fractions except in the case of smaller propellers. Therefore, it may be said that for larger propellers the mean wake fraction used in Froude's analysis can be obtained directly from the measured mean annular wakes, without conducting propeller open-water test. I think that the disagreement of two kinds of the effective mean wake fractions for smaller propellers would be mainly due to the defect of our method of propeller design for propellers to work in the eddying water behind ships. Such a defect of our method may be also seen in Fig. 22, where the revolutions of smaller propellers differ materially from those aimed at.

Since, as described in my paper entitled "Experiments on the Mutual Action between Propeller and Rudder,"⁽³⁾ the thrust and efficiency of a propeller are improved by a certain amount by the presence of a rudder at a short distance behind it, the effective mean wake fractions given in the previous table can not be said to be strictly correct. In general, for the purpose of obtaining the correct value of an effective mean wake fraction for a single-screw ship, the isolated propeller test in open water should be replaced by the open-water test of the propeller arranged in front of a rudder, and the expression of (4) should be modified, taking the effect of the rudder into consideration.

Lastly, I would like to state that, in order to obtain the theoretically more correct value of the effective mean wake fraction for a single-screw full-lined ship, by conducting an open-water test, this test should be made in turbulent water, not in still water. But the effective mean wake fraction thus obtained should not be used for the design of propellers by means of the propeller design diagrams, because these diagrams are those which summarized the results of systematic isolated propeller tests in still water.

Appendix III.

Analysis of Test Results by Froude's Method.

As stated before, propeller open-water tests are, as a general rule, not conducted at our Tank. But, utilising the results of the open-water tests, which had been carried out with the object of comparing the various kinds of mean wake fractions, the results of the self-propulsion tests were analysed by Froude's method, because the analysed results would be useful to other Tank experimenters for comparing these with their own data. The hull coefficients η_h , propeller efficiencies (behind) η_p' , propeller efficiencies (open) η_p and relative rotative coefficients η_r at 3,000 S.H.P. of 120-m. ships, associated with the propulsive coefficients η , thrust deduction fractions t and effective mean wake fractions w_a , are tabulated as follows.

⁽³⁾ Jour. Soc. N. A. Japan, Oct. 1933.

Comparison of the Analysed Results.								
Model No.	Propeller No.	η	t	w_a	η_h	η'_p	η_p	η_r
319	174	.83	.27	.41	1.24	.67	.60	1.12
195	155	.91	.17	.37	1.32	.69	.64	1.08
320	178	.89	.16	.34	1.27	.70	.64	1.09
319	175	.79	.28	.47	1.36	.58	.54	1.07
195	156	.85	.19	.42	1.40	.61	.57	1.07
320	179	.85	.16	.39	1.38	.62	.58	1.07
319	176	.75	.23	.52	1.50	.50	.47	1.06
195	157	.79	.19	.50	1.62	.49	.47	1.04
320	180	.81	.16	.45	1.53	.53	.51	1.04
319	177	.72	.28	.59	1.76	.41	.39	1.05
195	158	.73	.18	.52	1.71	.43	.42	1.02
320	181	.77	.15	.48	1.64	.47	.46	1.02

討 論

○會長(藤島範平君) 何方か御質問か、御意見は御座いませんか。

○出淵 巽君 大變結構な paper で私の最近見た中で最も面白いものゝ一つであります。158 頁の nominal mean wake と effective mean wake との difference でありますが、最近私達の方で 2 隻の船で、之に相當するものをやつたのですが、一つは effective mean wake に相當するもので behind and open tests をし、一つは其の propeller を current meter と見て open test で free に廻して、速力と回轉數との關係を求め、其の calibration curve より wake を出しました。其の兩方を比較しますと、speed length ratio が 0.7 位だと丁度此處に在る 4% 位の difference になりますが、次第に high speed になると差が小さくなり、1.3~1.5 位になると殆んど一致します。之れは理論的に考へたのではないが、實驗的に見て high speed になると大體一致しますが、之れに對して何か御考、若くは實驗があつたら御知らせ下さいませんか。

○山縣昌夫君 我々は殆んど low speed vessel のみで high speed のものは扱つた事はありませんから、此の 2 つの mean wake が high speed で合ふか合はぬか判りません。尤も一般に twin screw のものは良く合ひます。之れは wake の radial vibration が餘り無いからです。

○出淵 巽君 我々で test したのは、twin, triple, quadruple であります。有難う御座いました。

○會長(藤島範平君) 他にありませんか。……無い様ですから一言御禮申し上げます。山縣君は昨年來引續き御研究になつて居ります船體の後部と propeller との關係を、今日御發表下さいまし

て、誠に面白く拜聴致しました。逡信省に水槽が出来まして以來、段々と有益なる研究を御發表に相成り、其結果は船舶改善施設に依る新造船船の實際就航後の成績が拔群である事で證據立てられました事は、誠に喜ばしい次第であります。今日は志波、山縣兩君が響を並べて更に新研究を御發表になり、其の武者振り實に勇ましい事であります。逡信省の仕事としては此水槽試験所は、最も重要なものゝ一つとして我國の造船の進歩發達に貢献せらるゝ事は勿論、將來に於ては世界に於ける權威ある存在たるに至るべき事疑を容れないのでありますから、此上とも充分力を入れて豫算も充分に御取りになつて、更に研究を續けられん事を希望して諸君と共に拍手を以つて御禮申上げる次第であります。(一同拍手)

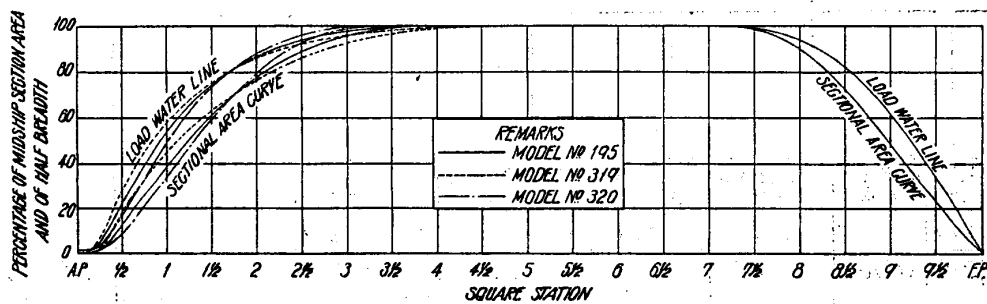
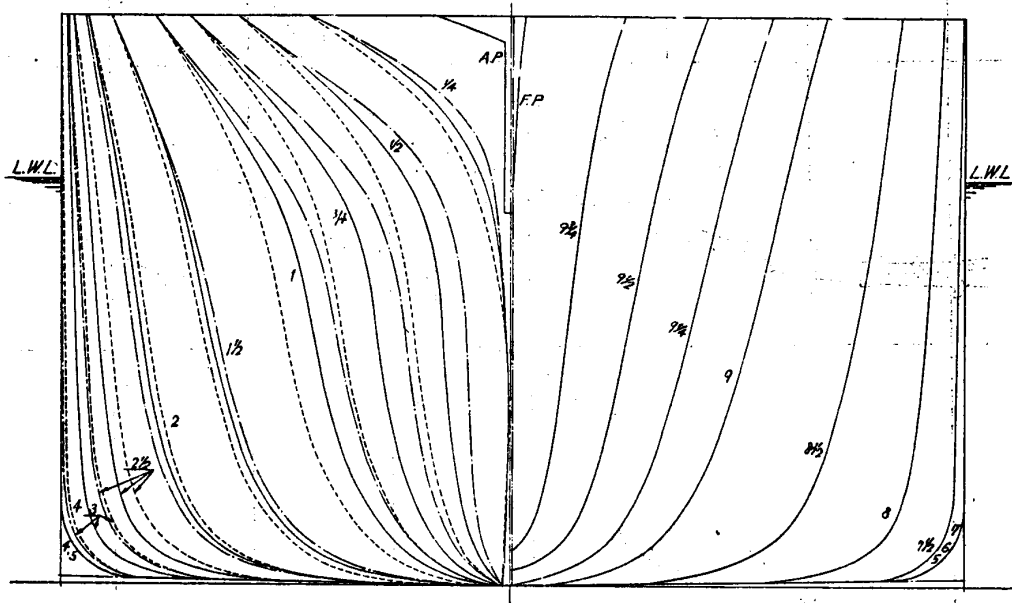


FIG. 1.— SECTIONAL AREA CURVES AND LOAD WATER LINES

SCALE OF MODEL 1 : 20
 LENGTH FP OF MODEL 6.000M
 BREADTH EXTREME 8.000M
 LOAD DRAUGHT 3.550M

MODEL NO 195
 MODEL NO 319
 MODEL NO 320

BODY PLANS



BOW AND STERN ARRANGEMENTS

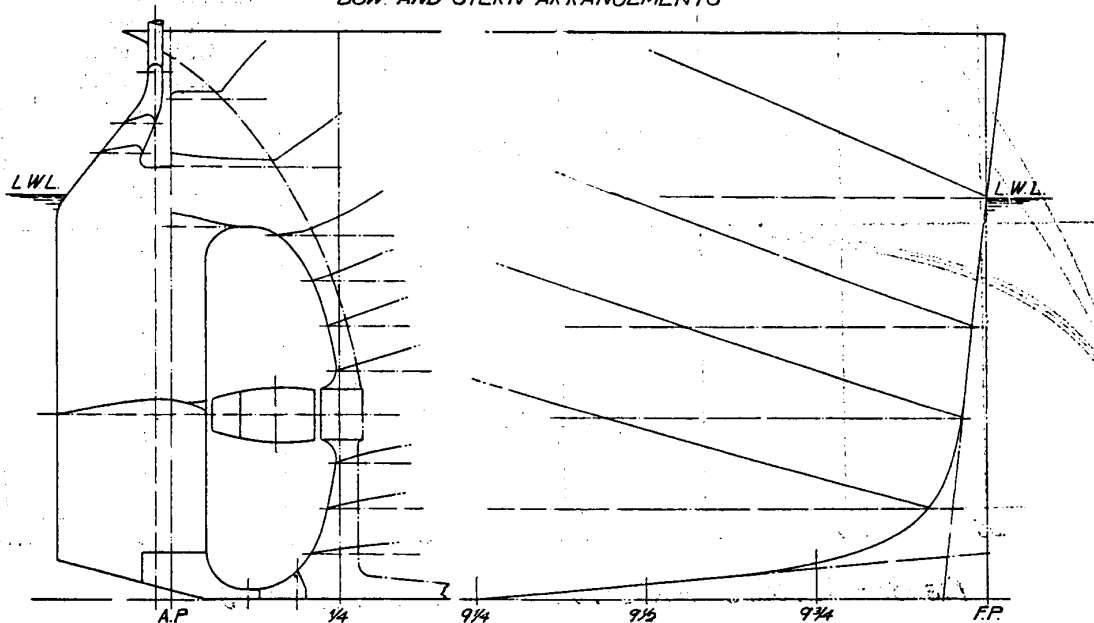


FIG. 2.— SHIP MODELS NO 195, 319 AND 320

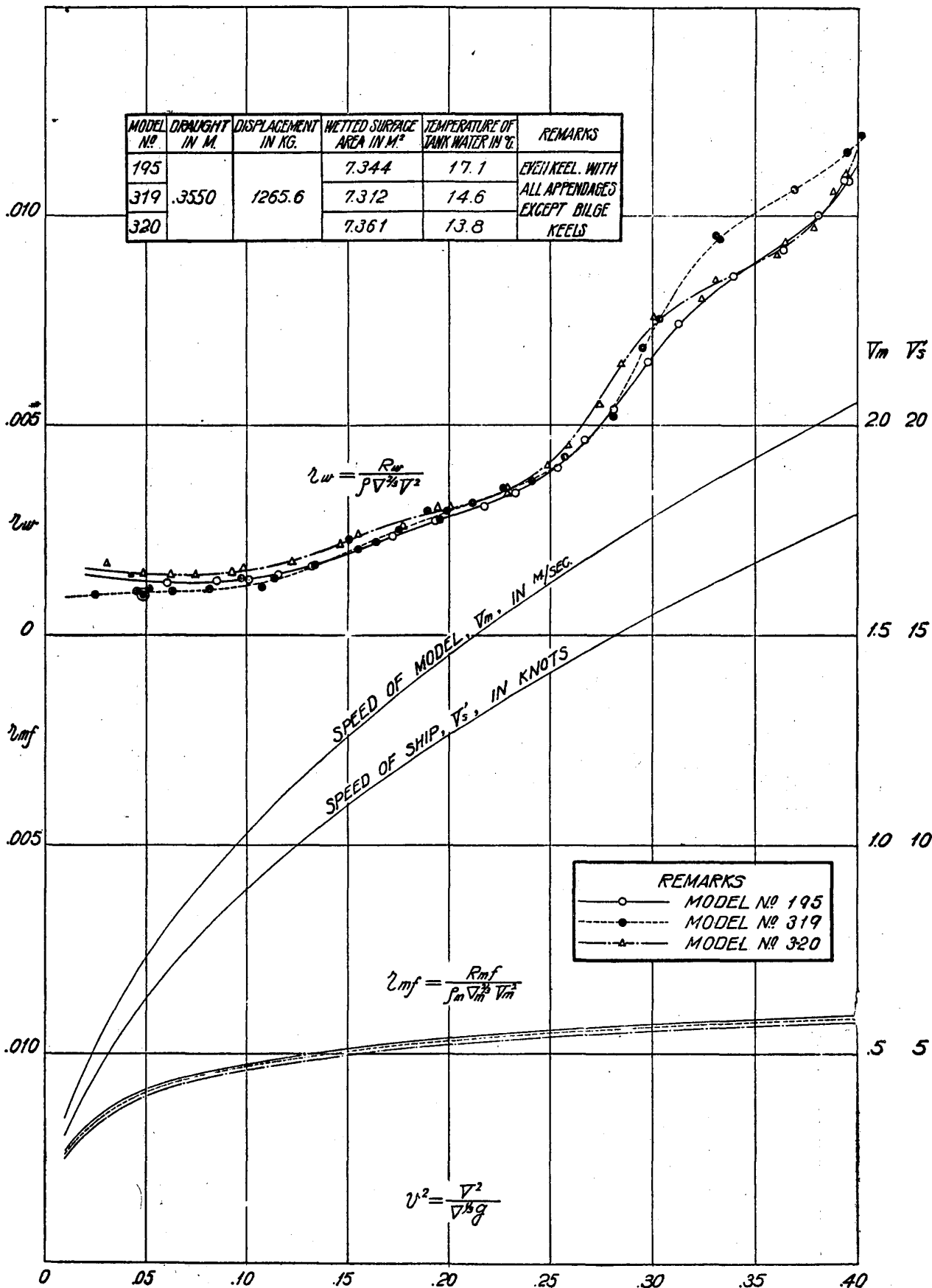


FIG. 3.—RESULTS OF RESISTANCE TESTS. $L_m = 6.000M.$

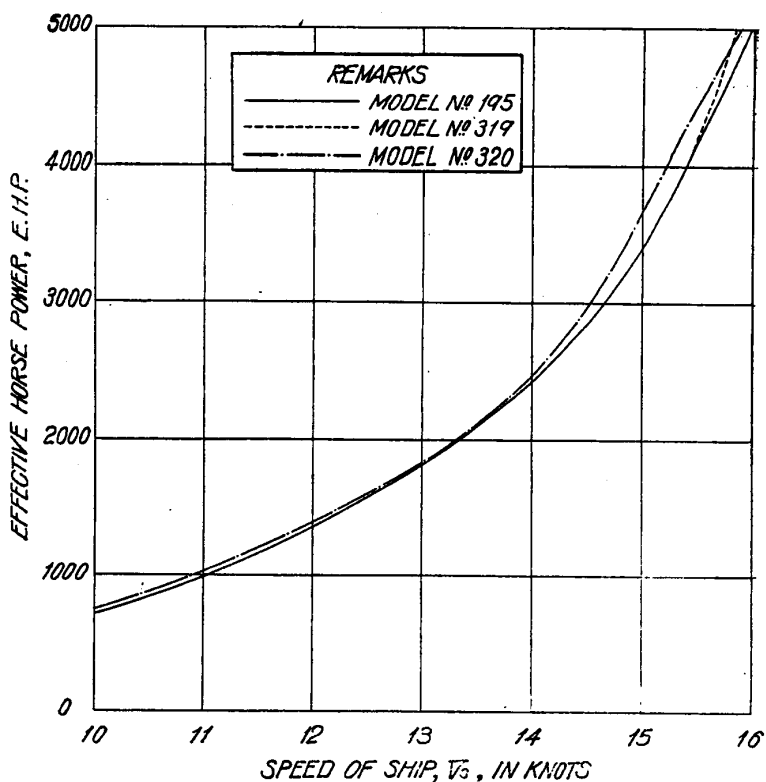


FIG. 4.—EFFECTIVE HORSE-POWER CURVES FOR 120M. VESSELS.

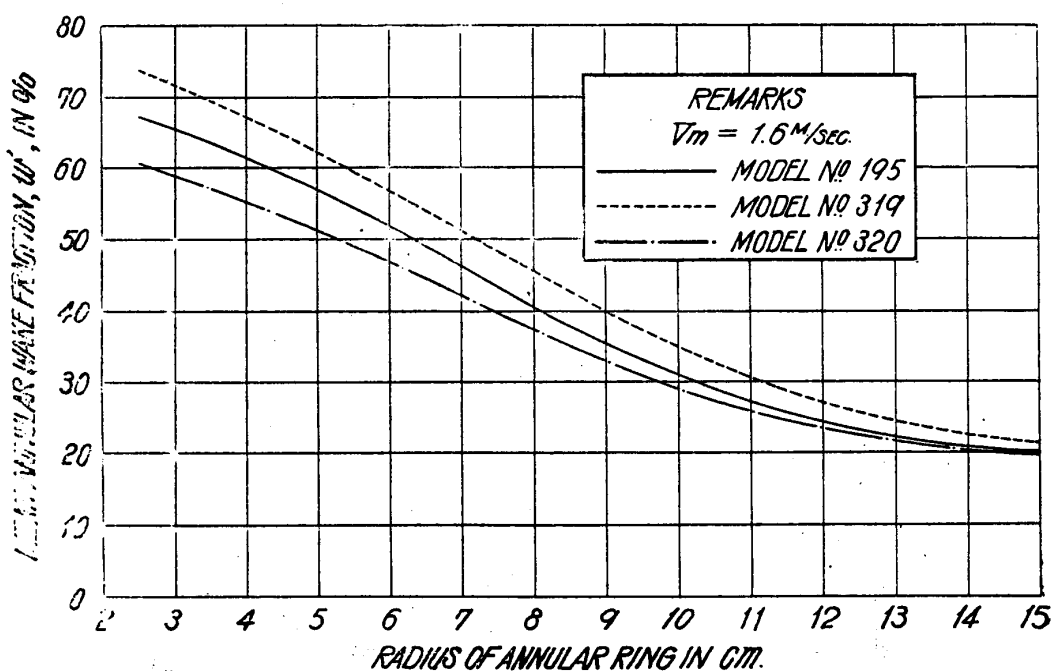


FIG. 5.—MEAN ANNULAR WAKE DISTRIBUTIONS MEASURED BY BLADE-WHEELS.

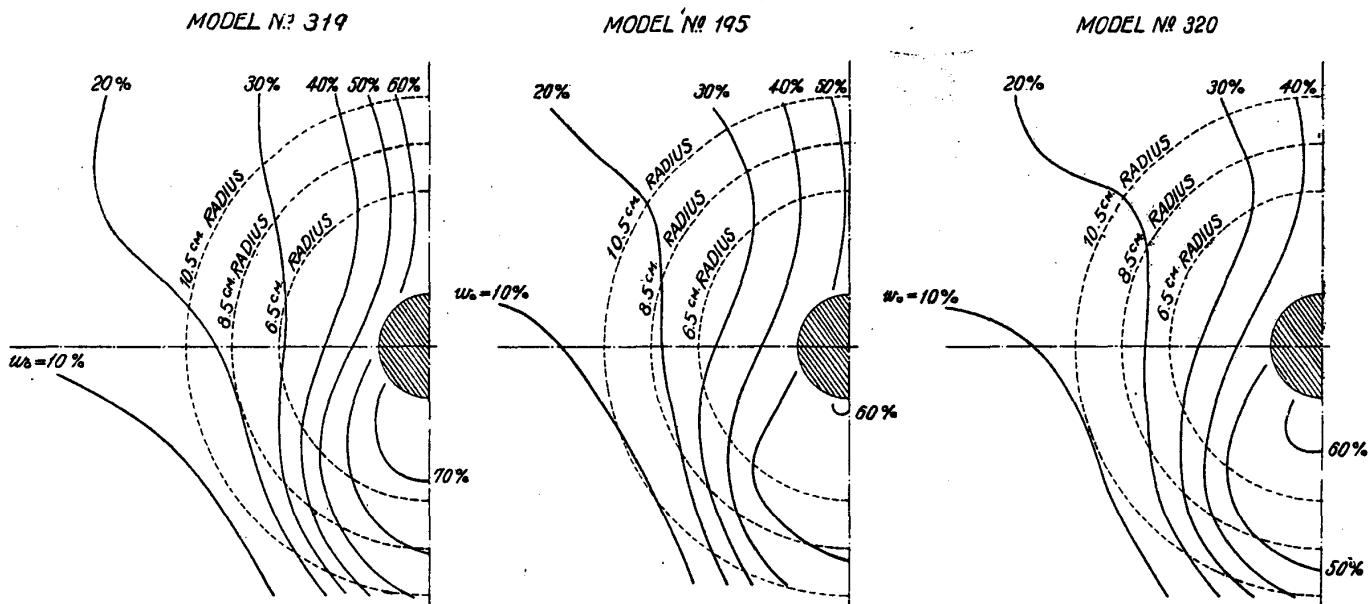


FIG. 6.—WAKE DISTRIBUTIONS MEASURED BY PITOT TUBES. $V_m = 1.6 \text{ M/sec}$.

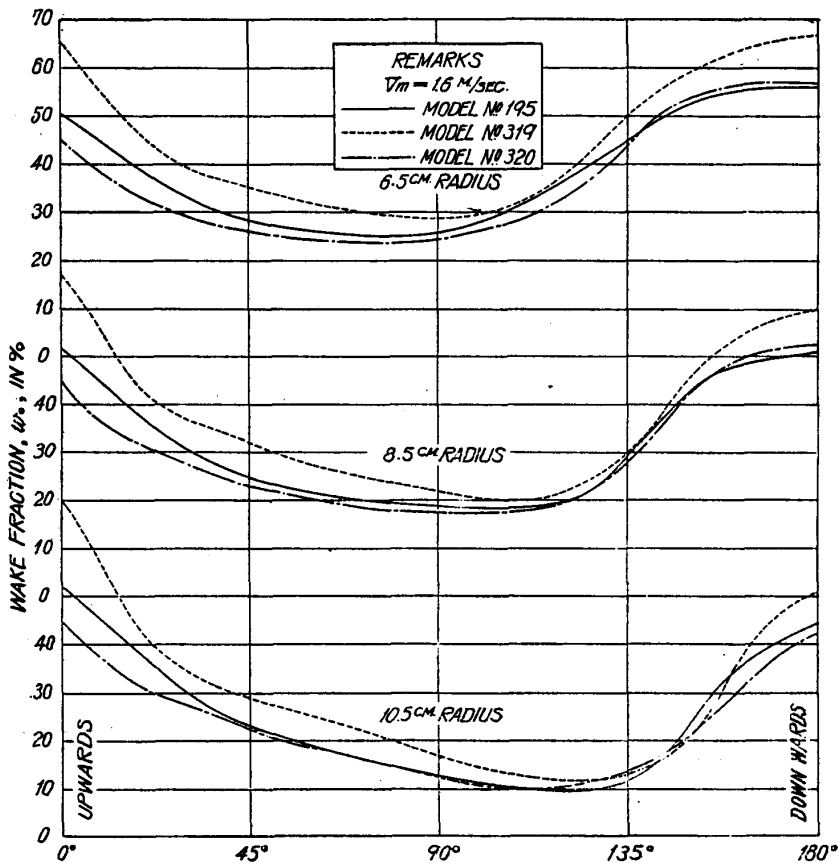


FIG. 7.—WAKE DISTRIBUTIONS OVER ANNULAR RINGS.

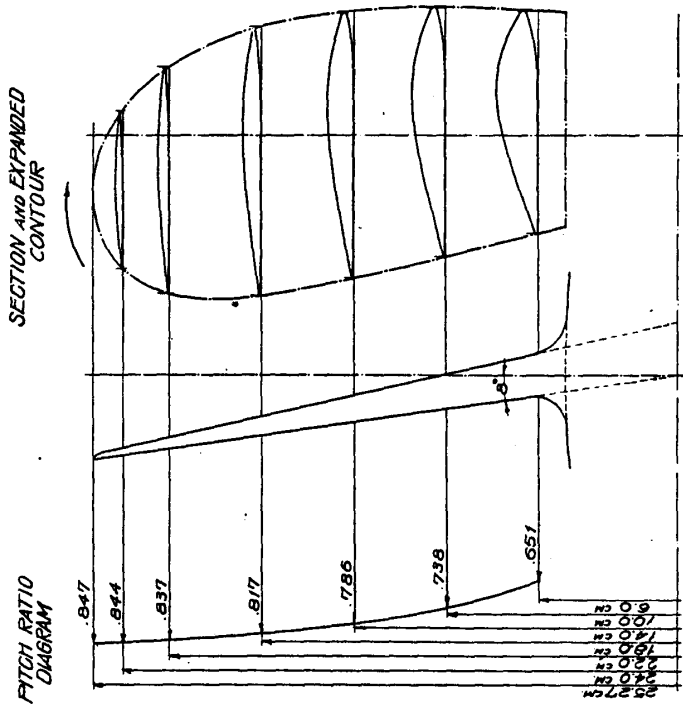


FIG. 9.—PROPELLER No. 175

DIAMETER	25.27 CM
BOSS RATIO	0.190
PITCH RATIO AT 0.7 R	0.815
EXPANDED AREA RATIO	0.407
BLADE THICKNESS RATIO	0.045
NUMBER OF BLADES	4

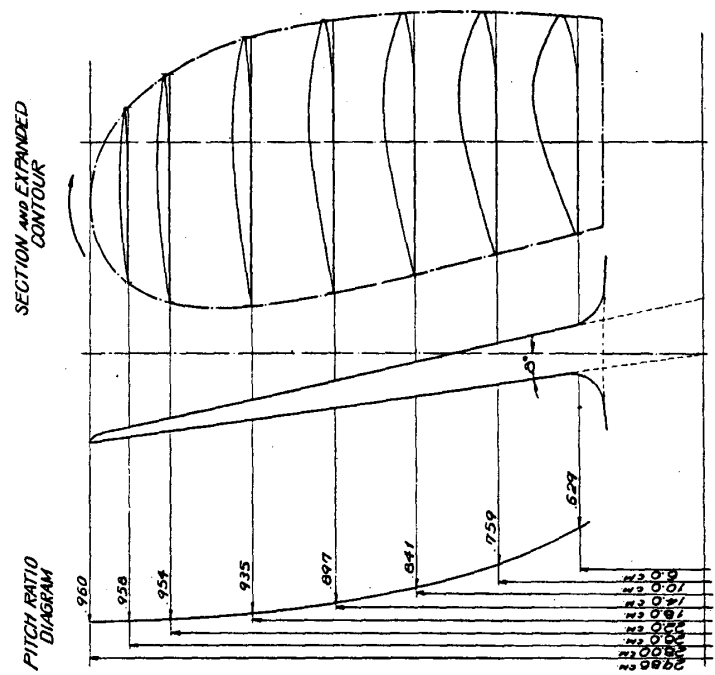


FIG. 8.—PROPELLER No. 174

DIAMETER	29.86 CM
BOSS RATIO	0.161
PITCH RATIO AT 0.7 R	0.927
EXPANDED AREA RATIO	0.407
BLADE THICKNESS RATIO	0.045
NUMBER OF BLADES	4

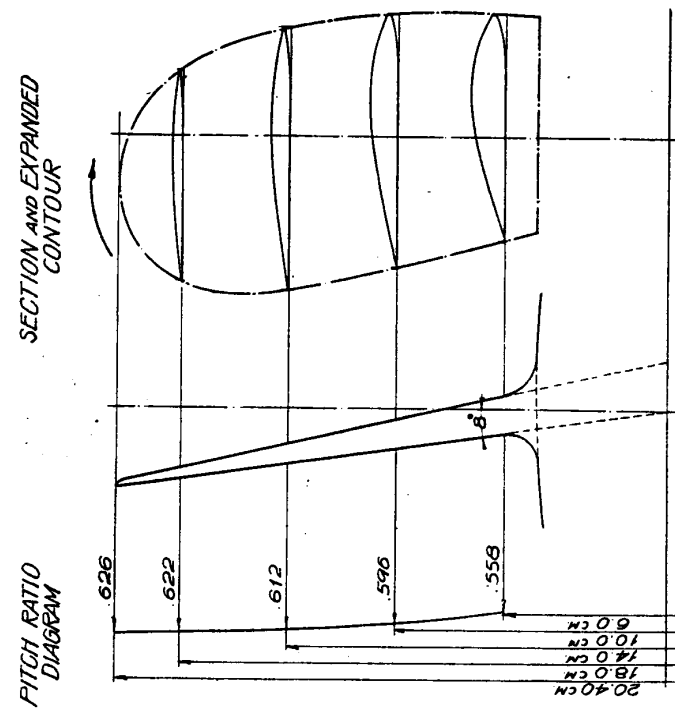


FIG 11.—PROPELLER No. 177

DIAMETER	20.40 CM
BOSS RATIO	0.235
PITCH RATIO AT 0.7 R	0.613
EXPANDED AREA RATIO	0.407
BLADE THICKNESS RATIO	0.045
NUMBER OF BLADES	4

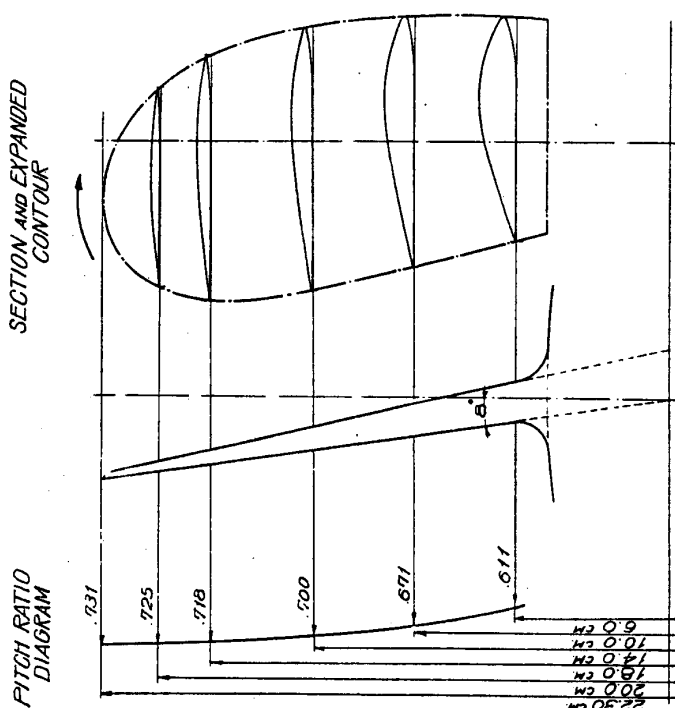


FIG. 10.—PROPELLER No. 176

DIAMETER	22.30 CM
BOSS RATIO	0.215
PITCH RATIO AT 0.7 R	0.709
EXPANDED AREA RATIO	0.407
BLADE THICKNESS RATIO	0.045
NUMBER OF BLADES	4

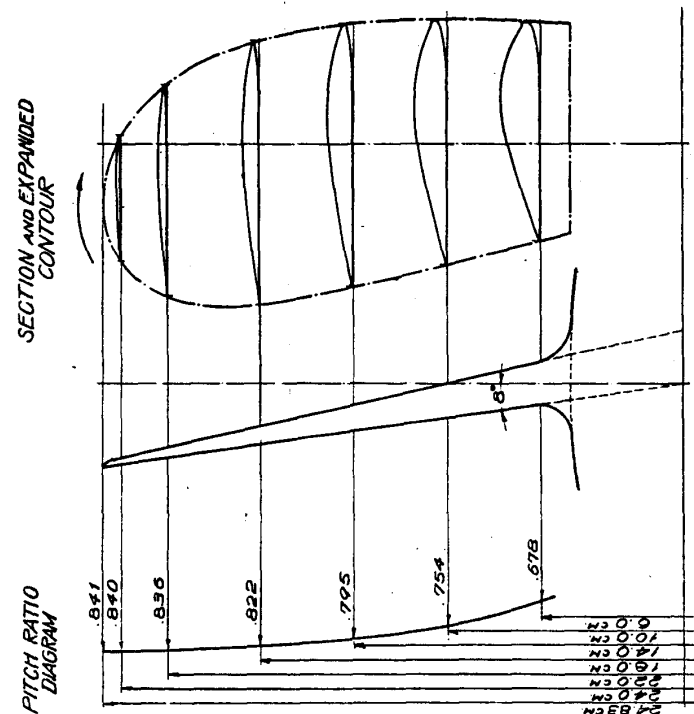


FIG. 13.—PROPELLER No. 179

DIAMETER	24.83 CM
BOSS RATIO	0.193
PITCH RATIO AT 0.7 R	0.818
EXPANDED AREA RATIO	0.407
BLADE THICKNESS RATIO	0.045
NUMBER OF BLADES	4

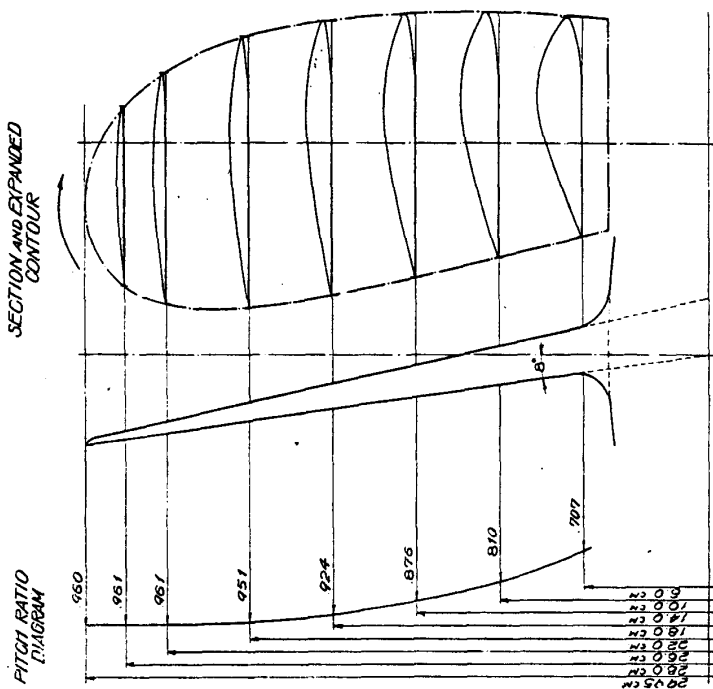


FIG. 12.—PROPELLER No. 178

DIAMETER	29.95 CM
BOSS RATIO	0.160
PITCH RATIO AT 0.7 R	0.946
EXPANDED AREA RATIO	0.407
BLADE THICKNESS RATIO	0.045
NUMBER OF BLADES	4

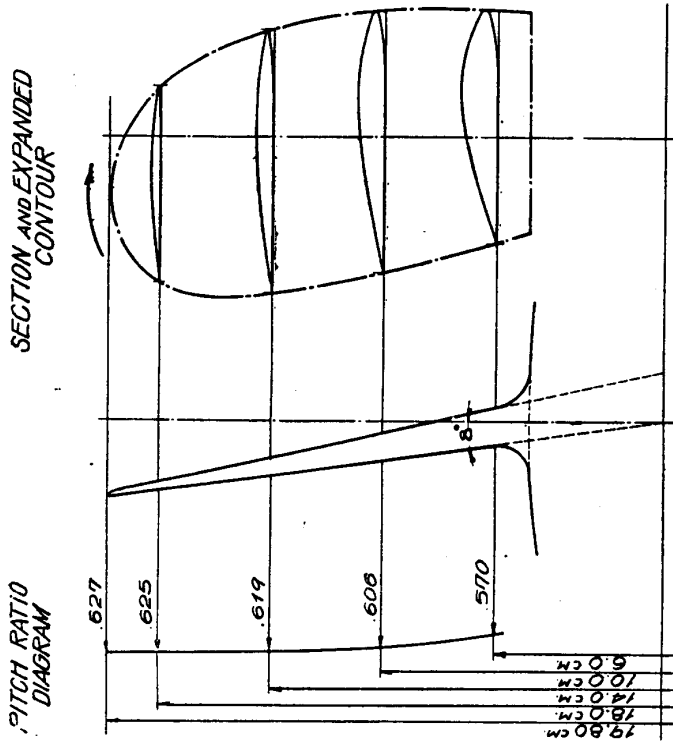


FIG. 15.—PROPELLER No. 181

DIAMETER	19.80 CM.
BOSS RATIO	0.242
PITCH RATIO AT 0.7 R	0.619
EXPANDED AREA RATIO	0.407
BLADE THICKNESS RATIO	0.045
NUMBER OF BLADES	4

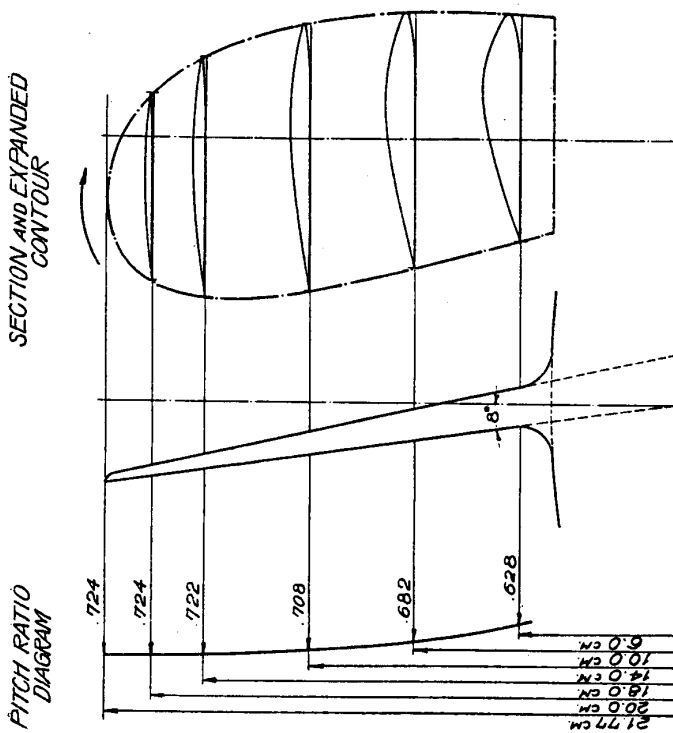


FIG. 14.—PROPELLER No. 180

DIAMETER	21.77 CM.
BOSS RATIO	0.221
PITCH RATIO AT 0.7 R	0.714
EXPANDED AREA RATIO	0.407
BLADE THICKNESS RATIO	0.045
NUMBER OF BLADES	4

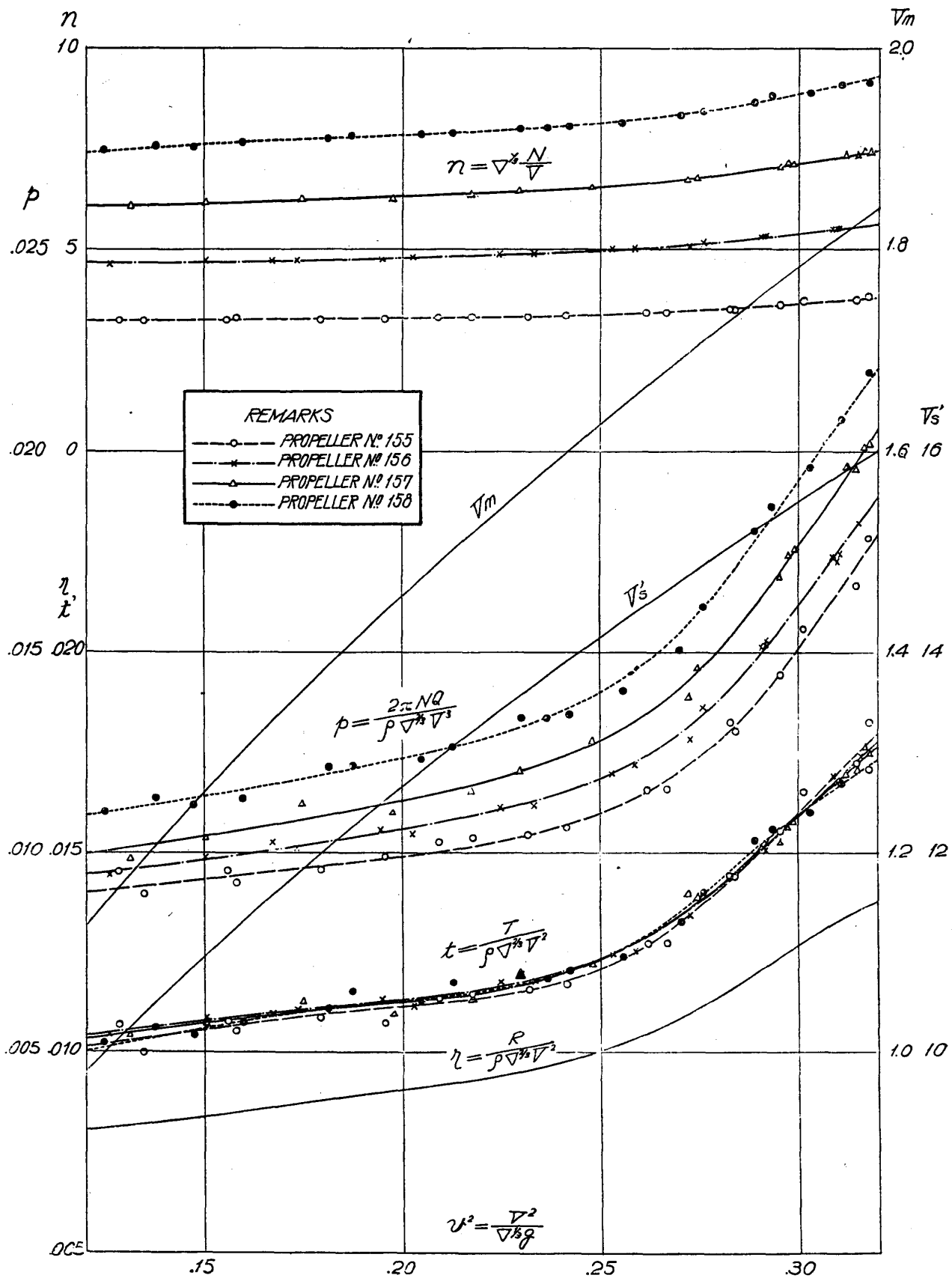


FIG. 16. - RESULTS OF SELF-PROPULSION TESTS OF MODEL N^o 195.

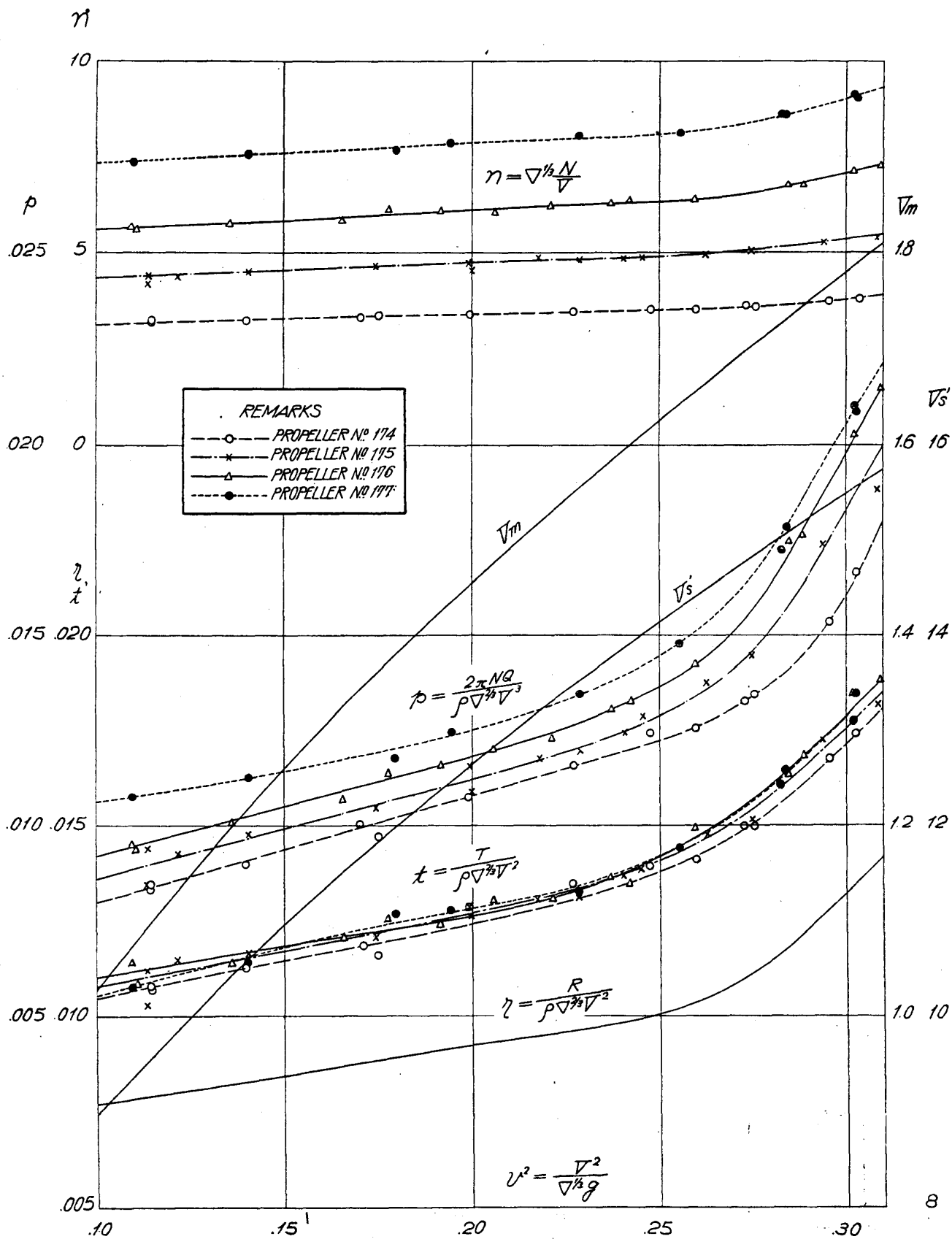


FIG. 17. — RESULTS OF SELF-PROPULSION TESTS OF MODEL NO. 319

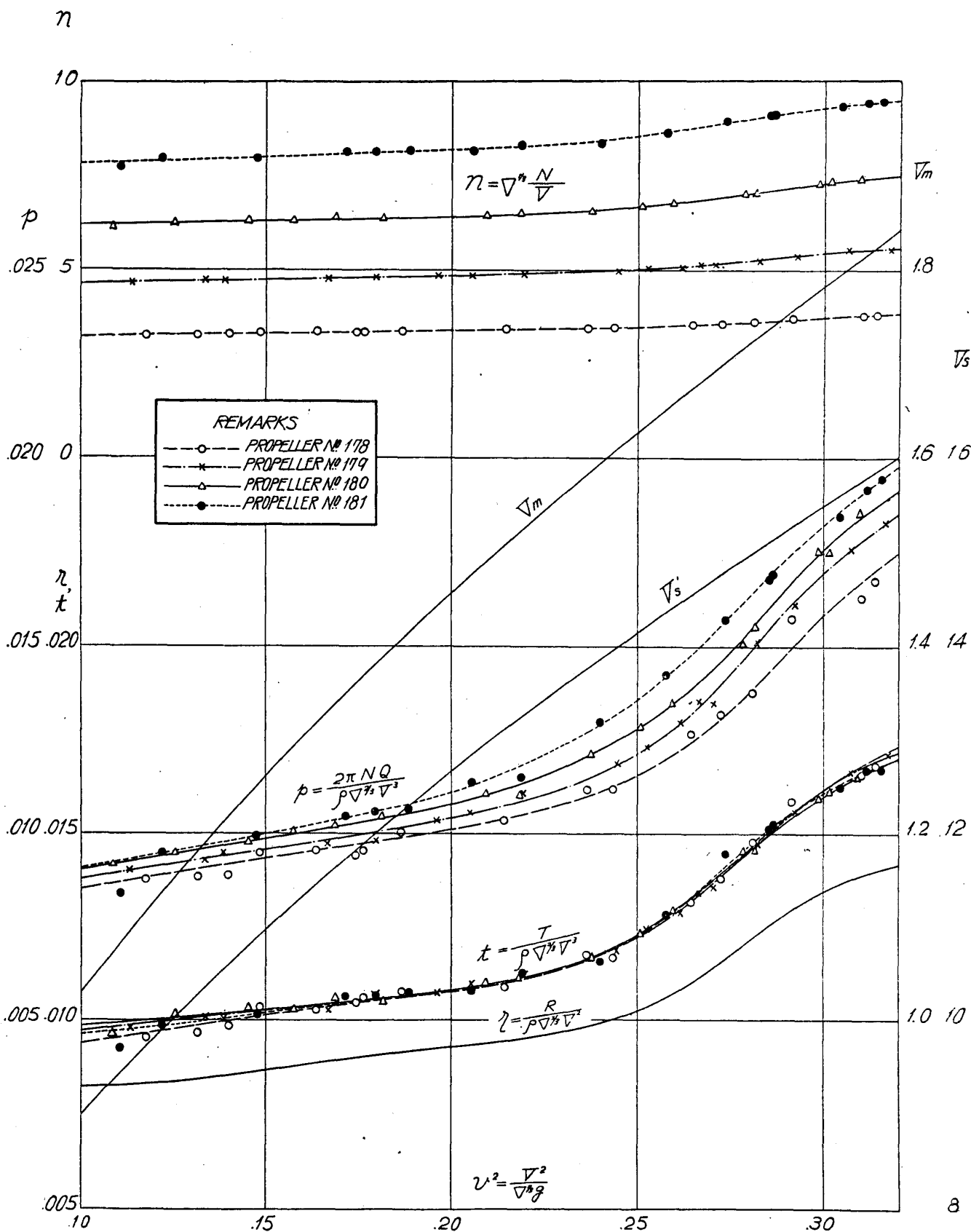


FIG. 18. — RESULTS OF SELF-PROPULSION TESTS OF MODEL NO. 320.

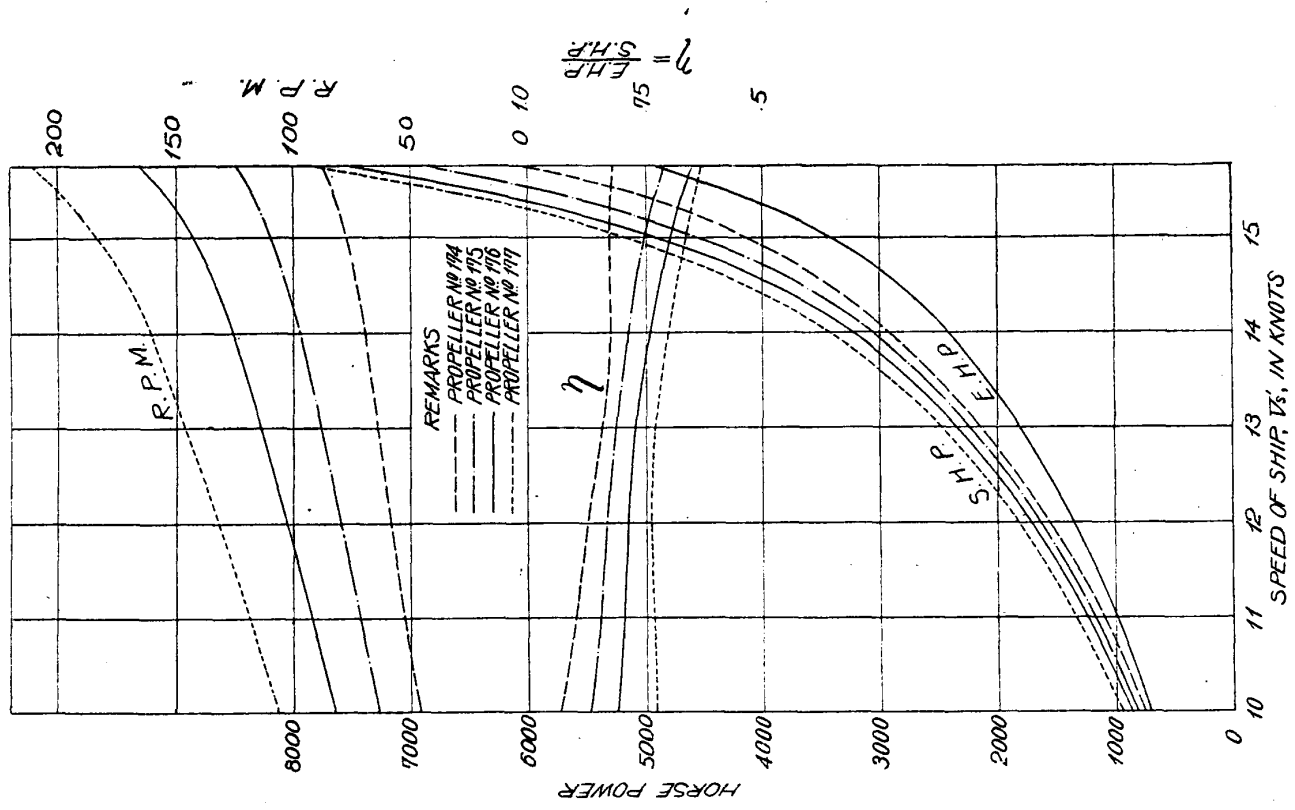


FIG. 20.—S.H.P., R.P.M. AND η CURVES FOR 120-M VESSEL (MODEL NO. 319)

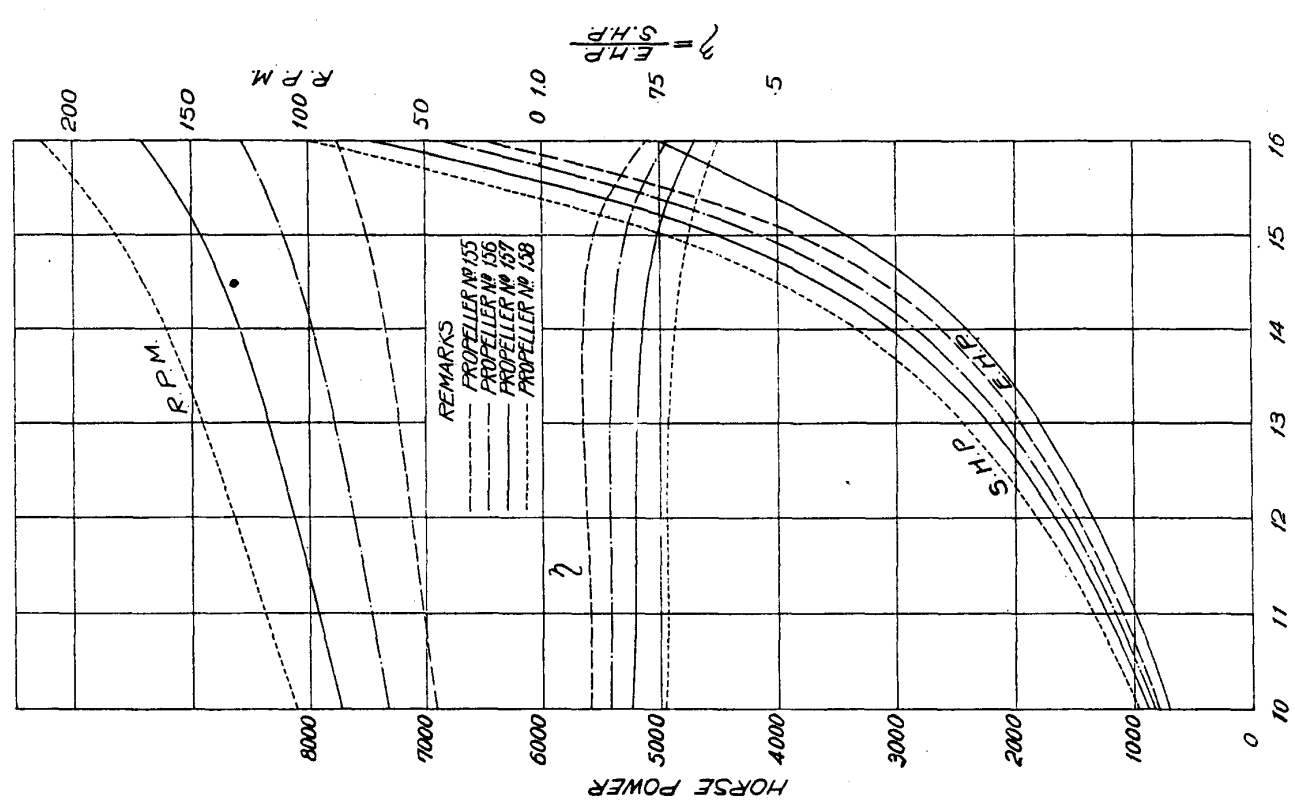


FIG. 19.—S.H.P., R.P.M. AND η CURVES FOR 120-M VESSEL (MODEL NO. 195)

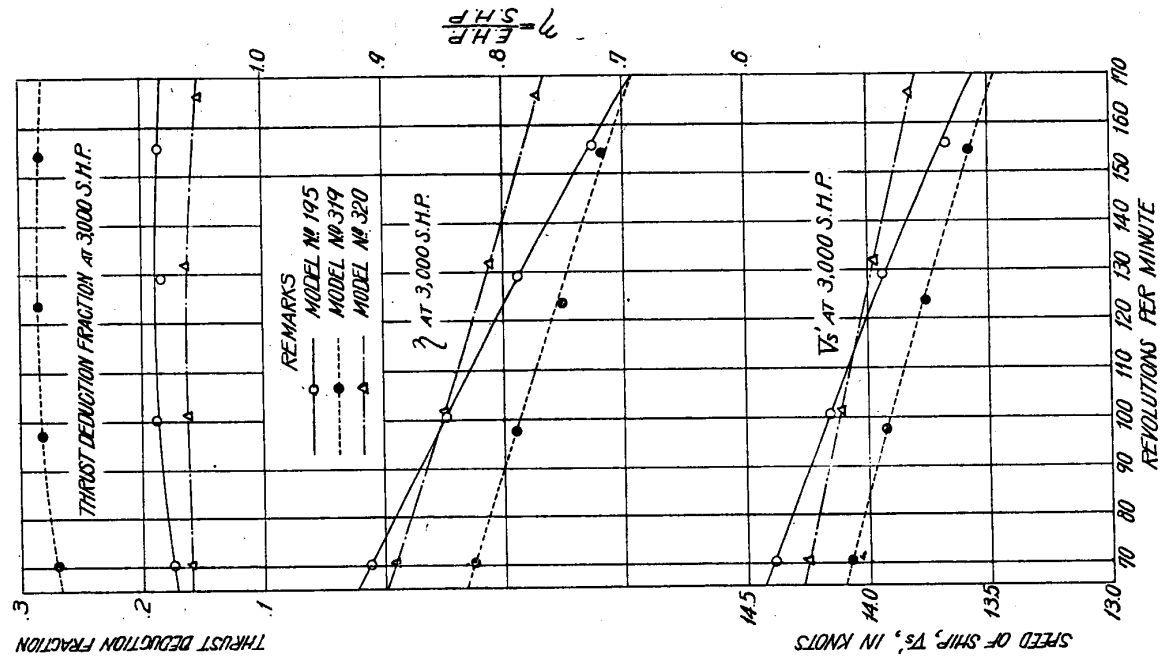


FIG. 22.—ESTIMATED RESULTS AT 3,000 S.H.P. ON A BASE OF R.P.M.

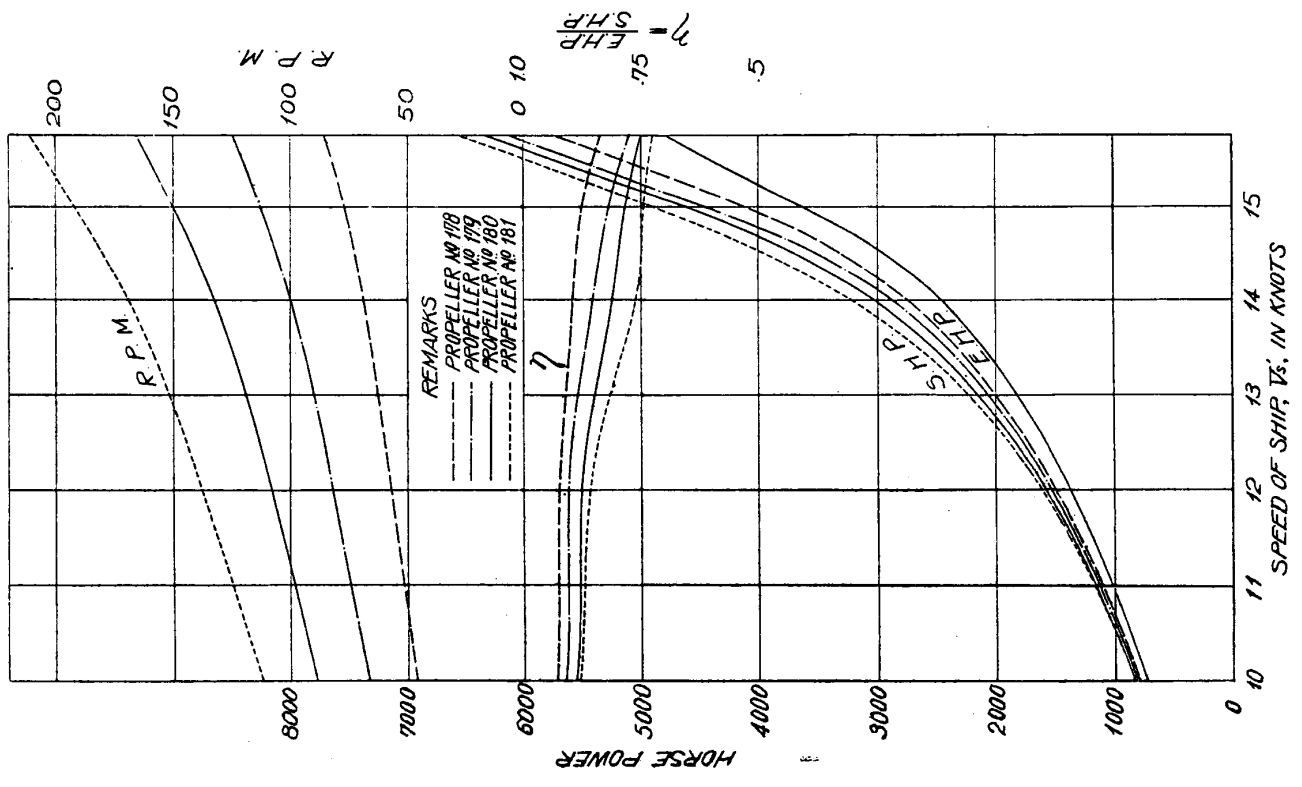


FIG. 21.—S.H.P., R.P.M. AND η CURVES FOR 120-M VESSEL. (MODEL NO. 320.)

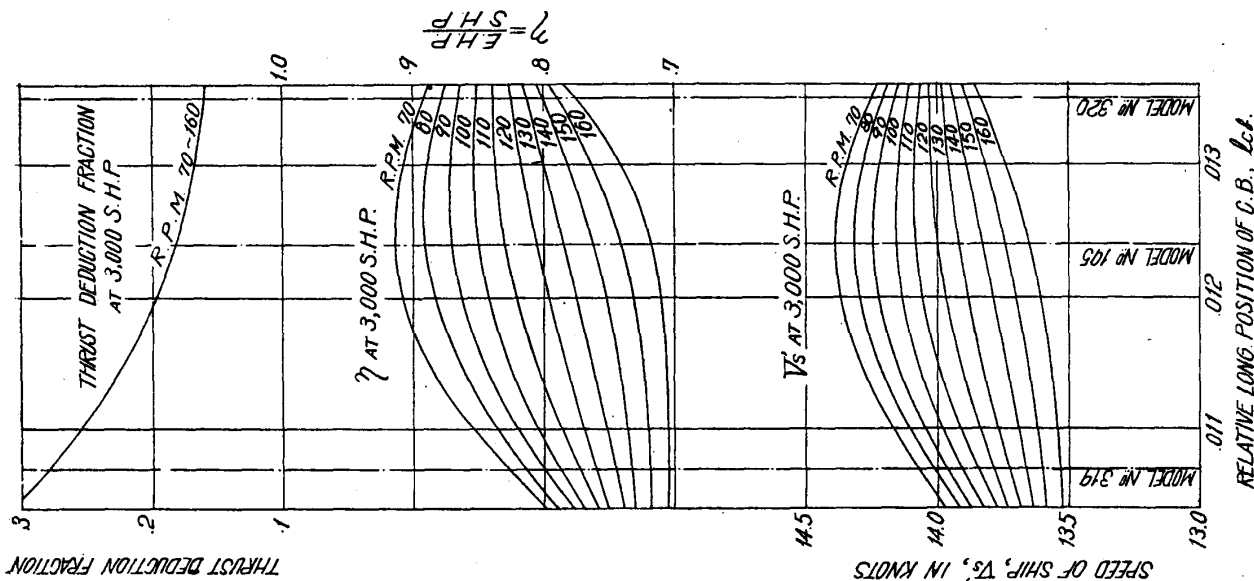


FIG. 23.—ESTIMATED RESULTS AT 3,000 S.H.P. ON A BASE OF L_{ct} .

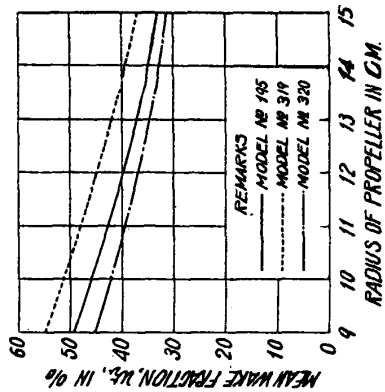


FIG. 26.—MEAN WAKE FRACTIONS CALCULATED BY VOLUME-INTEGRATION ON A BASE OF PROPELLER RADIUS.

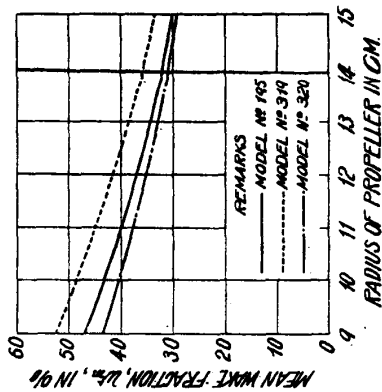


FIG. 27.—MEAN WAKE FRACTIONS CALCULATED BY MOMENTUM-INTEGRATION ON A BASE OF PROPELLER RADIUS.

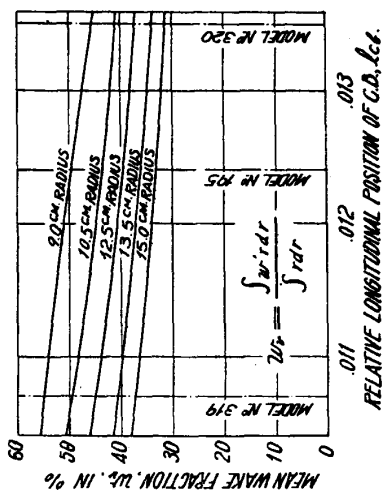


FIG. 24.—MEAN WAKE FRACTIONS CALCULATED BY VOLUME-INTEGRATION ON A BASE OF L_{ct} .

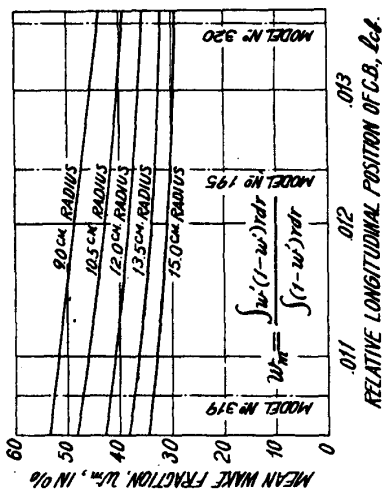


FIG. 25.—MEAN WAKE FRACTIONS CALCULATED BY MOMENTUM-INTEGRATION ON A BASE OF L_{ct} .